

Coaxial-disk flow and flow about a rotating disk of a Maxwellian fluid

By N. PHAN-THIEN†

Department of Mechanical Engineering, University of Sydney, N.S.W. 2006, Australia

(Received 1 July 1982 and in revised form 28 September 1982)

The flows of a Maxwellian fluid between two rotating coaxial disks and about a rotating disk are discussed. Asymptotic solutions are derived and numerical solutions are reported for a Weissenberg number up to 10 and a Reynolds number of up to 50. The solutions show transverse wave propagation. Also, at low Weissenberg number the moment coefficient for a rotating disk wetted on both sides is inversely proportional to the square root of the angular velocity of the disk. At high Weissenberg number it is inversely proportional to the angular velocity of the disk. The transition occurs at a Weissenberg number of unity.

1. Introduction

We consider the flow of a viscoelastic fluid between two rotating parallel and infinite coaxial disks. The flow is of considerable interest to rheologists in that it models the dynamics of the so-called ‘parallel-plate viscometer’ (Walters 1975). The corresponding problem for a Newtonian fluid has a long history, dated back to the Kármán solution (Kármán 1921) and has been discussed by Cochran (1934), Batchelor (1951), Stewartson (1953) and Benton (1966). At high Reynolds number (based on the gap thickness) it is known that there are bifurcation points (Holodniok, Kubíček & Hlaváček 1977), but we are not concerned with this aspect of the problem.

The corresponding flow problems for non-Newtonian fluids have been considered by various authors. Rathna (1962) used the momentum-integral method to investigate the flow of a second-order fluid about an infinite rotating disk. Her results have been criticized by Williams (1976) in that they predict a flow reversal at a sufficiently large distance from the disk. Williams also gave perturbation solutions (in terms of the Weissenberg number) to the flow of a second-order fluid and an Oldroyd fluid B about an infinite rotating disk. For the range of parameter values used, he concluded that there is only a slight departure from Newtonian behaviour, although the small-time analysis indicates some marked transient non-Newtonian effects in the early development of the flow. The steady coaxial-disk flow has been considered by Griffiths, Jones & Walters (1969), using a third-order fluid model, by Bhatnagar & Zago (1978), using a second-order fluid model, and recently by Bhatnagar & Perera (1982) using an Oldroyd 4-constant model. However, in the latter reference the stress representation reported by Bhatnagar & Perera can only be considered as truncated power series in the radial coordinate – we will return to this point later – and it is not known of the error involved in leaving out terms $O(r^3)$ and higher in the stress representation.

In this paper we consider the flow problems for a Maxwellian fluid. It will be shown

† Present address: Department of Chemical Engineering, Caltech, Pasadena, CA 91125.

that there exist exact solutions, in the sense that the governing equations can be reduced to a set of quadratures in the z -coordinate at steady state, or to a set of partial differential equations in the z - and t -coordinate. Three cases will be discussed: when one disk is at rest, when both disks are rotating in the same direction and when the distance between the disks is infinitely large (flow about a rotating disk). Appropriate asymptotic solutions are developed for these cases. Full numerical solutions are also reported for a Weissenberg number up to 10 and a Reynolds number up to 50. Our choice of the constitutive model is motivated by the fact that, aside from its being capable of having exact solutions for the flow problems considered, most numerical schemes (finite-element or otherwise) employing the Maxwellian model do not converge at all at a global Weissenberg number exceeding a critical value of the order of unity (Pearson 1982). It is not known whether this lack of convergence is due inherently to the model or to the numerical scheme employed. Having an exact solution in a non-trivial flow geometry at least enables one to trace back the working of the computer program. Hopefully this will shed additional insight into an otherwise untractable problem. Furthermore, the Maxwellian model does describe most observed non-Newtonian effects qualitatively, at least for the so-called Boger's fluid (a dilute solution of polyacrylamide in a mixture of water and maltose syrup – Boger 1977/78) at steady flow conditions. The conclusions of this paper are expected to apply to those fluids.

2. Formulation

The problem we are concerned with is that of a viscoelastic fluid contained between two parallel coaxial disks. The bottom plate rotates at angular velocity Ω_1 and the top plate rotates at angular velocity Ω_2 . Both plates are set in motion at the instant of $t = 0+$. The thickness of the lubricant film is d . The fluid is assumed to be incompressible, so that $\nabla \cdot \mathbf{u} = 0$, and the equation of motion is $\nabla \cdot \boldsymbol{\sigma} = \rho D\mathbf{u}/Dt$, where \mathbf{u} is the velocity vector, $\boldsymbol{\sigma}$ is the stress, ρ is the density of the fluid and D/Dt is the material time derivative. Body forces are ignored here. The constitutive equation for the fluid is written in terms of the extra stress tensor \mathbf{S} , where $\boldsymbol{\sigma} = \mathbf{S} - P\mathbf{I}$, P being the pressure and \mathbf{I} the unit tensor. The lubricant is assumed to be a Maxwellian fluid; that is, if the velocity gradient is $\mathbf{L} = \nabla\mathbf{u}^T$ and the strain rate is $\mathbf{D} = \frac{1}{2}(\mathbf{L} + \mathbf{L}^T)$, where T denotes a transpose, then the extra stress \mathbf{S} is given by

$$\mathbf{S} + \lambda(\partial_t \mathbf{S} + \mathbf{u} \cdot \nabla \mathbf{S} - \mathbf{L}\mathbf{S} - \mathbf{S}\mathbf{L}^T) = 2\eta\mathbf{D}, \quad (1)$$

in which λ is the relaxation time and η is the viscosity of the liquid. Using a cylindrical coordinate system (r, θ, z) with the origin fixed at the centre of the bottom plate, and z the axis of symmetry, the relevant boundary conditions for the velocity field $\mathbf{u} = (u, v, w)$ are

$$\left. \begin{aligned} u = w = 0, \quad v = r\Omega_1 \quad (z = 0), \\ u = w = 0, \quad v = r\Omega_2 \quad (z = d). \end{aligned} \right\} \quad (2)$$

For time $t < 0$, both disks are at rest and we assume that

$$\mathbf{u}(\mathbf{x}, t) = 0 \quad (-\infty < t < 0, \quad \text{all } \mathbf{x}).$$

It will be shown that the classical solution of Kármán (1921), where

$$\mathbf{u} = (r\partial_z H, rG, -2H), \quad (3)$$

still holds. In (3) H and G are functions of z and t , both to be determined. When (3) is substituted in the constitutive relation (1) we obtain for the stresses

$$\begin{aligned} S_{rr} + \lambda(\partial_t S_{rr} + r \partial_z H \partial_r S_{rr} - 2H \partial_z S_{rr} - 2S_{rr} \partial_z H - 2r S_{rz} \partial_{zz} H) &= 2\eta \partial_z H, \\ S_{r\theta} + \lambda(\partial_t S_{r\theta} + r \partial_z H \partial_r S_{r\theta} - 2H \partial_z S_{r\theta} - 2S_{r\theta} \partial_z H - r S_{z\theta} \partial_{zz} H - r S_{rz} \partial_z G) &= 0, \\ S_{rz} + \lambda(\partial_t S_{rz} + r \partial_z H \partial_r S_{rz} - 2H \partial_z S_{rz} + S_{rz} \partial_z H - r S_{zz} \partial_{zz} H) &= \eta r \partial_{zz} H, \\ S_{\theta\theta} + \lambda(\partial_t S_{\theta\theta} + r \partial_z H \partial_r S_{\theta\theta} - 2H \partial_z S_{\theta\theta} - 2S_{z\theta} \partial_z H - 2r S_{z\theta} \partial_z G) &= 2\eta \partial_z H, \\ S_{z\theta} + \lambda(\partial_t S_{z\theta} + r \partial_z H \partial_r S_{z\theta} - 2H \partial_z S_{z\theta} + S_{z\theta} \partial_z H - r S_{zz} \partial_z G) &= \eta r \partial_z G, \\ S_{zz} + \lambda(\partial_t S_{zz} + r \partial_z H \partial_r S_{zz} - 2H \partial_z S_{zz} + 4S_{zz} \partial_z H) &= -4\eta \partial_z H. \end{aligned}$$

2.1. Coaxial-disk flow

When both disks are rotating at different angular velocities, we find it convenient to non-dimensionalise z by the film thickness d , and time t by $\Omega_2 - \Omega_1$, viz

$$\zeta = \frac{z}{d}, \quad \tau = (\Omega_2 - \Omega_1)t.$$

Furthermore, the velocities can be non-dimensionalized according to

$$\begin{aligned} G(z, t) &= (\Omega_2 - \Omega_1)g(\zeta, \tau) + \Omega_1, \\ H(z, t) &= (\Omega_2 - \Omega_1)dh(\zeta, \tau). \end{aligned}$$

In terms of these dimensionless variables, it is found that a possible representation of the stresses is†

$$\begin{aligned} S_{rr} &= \eta(\Omega_2 - \Omega_1) \left[\widehat{R}\widehat{R}_0 + \frac{r^2}{d^2} \widehat{R}\widehat{R}_1 \right], \\ S_{r\theta} &= \eta(\Omega_2 - \Omega_1) \frac{r^2}{d^2} \widehat{R}\widehat{\theta}, \\ S_{rz} &= \eta(\Omega_2 - \Omega_1) \frac{r}{d} \widehat{R}\widehat{Z}, \\ S_{\theta\theta} &= \eta(\Omega_2 - \Omega_1) \left[\widehat{\theta}\widehat{\theta}_0 + \frac{r^2}{d^2} \widehat{\theta}\widehat{\theta}_1 \right], \\ S_{\theta z} &= \eta(\Omega_2 - \Omega_1) \frac{r}{d} \widehat{\theta}\widehat{Z}, \\ S_{zz} &= \eta(\Omega_2 - \Omega_1) \widehat{Z}\widehat{Z}, \end{aligned}$$

where \widehat{ij} ; $i, j = (R, \theta, Z)$ are functions of ζ and τ and are given by

$$\widehat{R}\widehat{R}_0 + Wi(\widehat{R}\widehat{R}_0 - 2h\widehat{R}\widehat{R}'_0 - 2h'\widehat{R}\widehat{R}_0) = 2h', \tag{4}$$

$$\widehat{R}\widehat{R}_1 + Wi(\widehat{R}\widehat{R}_1 - 2h\widehat{R}\widehat{R}'_1 - 2h''\widehat{R}\widehat{Z}) = 0, \tag{5}$$

$$\widehat{R}\widehat{\theta} + Wi(\widehat{R}\widehat{\theta} - 2h\widehat{R}\widehat{\theta}' - h''\widehat{Z}\widehat{\theta} - g'\widehat{R}\widehat{Z}) = 0, \tag{6}$$

$$\widehat{R}\widehat{Z} + Wi(\widehat{R}\widehat{Z} - 2h\widehat{R}\widehat{Z}' + 2h'\widehat{R}\widehat{Z} - h''\widehat{Z}\widehat{Z}) = h'', \tag{7}$$

$$\widehat{\theta}\widehat{\theta}_0 + Wi(\widehat{\theta}\widehat{\theta}_0 - 2h\widehat{\theta}\widehat{\theta}'_0 - 2h'\widehat{\theta}\widehat{\theta}_0) = 2h', \tag{8}$$

† This stress representation can be derived directly from the history of the particle path, using (3) and the equivalent integral Maxwellian model.

$$\widehat{\theta}\widehat{\theta}_1 + Wi(\widehat{\theta}\widehat{\theta}_1 - 2h\widehat{\theta}\widehat{\theta}'_1 - 2g'\widehat{Z}\widehat{\theta}) = 0, \tag{9}$$

$$\widehat{\theta}\widehat{Z} + Wi(\widehat{\theta}\widehat{Z} - 2h\widehat{\theta}\widehat{Z}' + 2h'\widehat{\theta}\widehat{Z} - g'\widehat{Z}\widehat{Z}) = g', \tag{10}$$

$$\widehat{Z}\widehat{Z} + Wi(\widehat{Z}\widehat{Z} - 2h\widehat{Z}\widehat{Z}' + 4h'\widehat{Z}\widehat{Z}) = -4h'. \tag{11}$$

In (4)–(11) Wi is the Weissenberg number defined by

$$Wi = \lambda(\Omega_2 - \Omega_1),$$

and we have used the shorthand notation (\cdot) and $(\cdot)'$ for τ - and ζ -derivatives respectively. Note that the stress representation is identical with that of Williams (1976), who considered an Oldroyd B -fluid, except that in the latter a quadratic term in r is required in S_{zz} . Conservation of linear momentum requires

$$\frac{\partial P}{\partial r} = \eta(\Omega_2 - \Omega_1) \frac{r}{d^2} \{3\widehat{R}\widehat{R}_1 - \widehat{\theta}\widehat{\theta}_1 + \widehat{R}\widehat{Z}' - Re[h' + h'^2 - (g + \omega) - (g + \omega)^2 - 2hh'']\}$$

in the radial direction,

$$\frac{1}{r} \frac{\partial P}{\partial \theta} = \eta(\Omega_2 - \Omega_1) \frac{r}{d^2} \{4\widehat{R}\widehat{\theta} + \widehat{\theta}\widehat{Z}' - Re[\dot{g} + 2h'(g + \omega) = 2hg']\} \text{ in the } \theta\text{-direction,}$$

$$\frac{\partial P}{\partial z} = \eta(\Omega_2 - \Omega_1) \frac{1}{d} \{2\widehat{R}\widehat{Z} + \widehat{Z}\widehat{Z}' + 2Re[h + 2hh']\} \text{ in the } z\text{-direction.}$$

Axisymmetry requires that

$$4\widehat{R}\widehat{\theta} + \widehat{\theta}\widehat{Z}' - Re[\dot{g} + 2h'(g + \omega) - 2hg'] = 0. \tag{12}$$

Compatibility between $\partial_z P$ and $\partial_r P$ requires that

$$\begin{aligned} p &= \frac{\partial_r P}{\eta(\Omega_2 - \Omega_1) r/d^2} \\ &= 3\widehat{R}\widehat{R}_1 - \widehat{\theta}\widehat{\theta}_1 + \widehat{R}\widehat{Z}' - Re[h' + h'^2 - (g + \omega)^2 - 2hh''] \end{aligned} \tag{13}$$

is a function of time only. Alternatively

$$3\widehat{R}\widehat{R}'_1 - \widehat{\theta}\widehat{\theta}'_1 + \widehat{R}\widehat{Z}'' - Re[h'' - 2(g + \omega)g' - 2hh'''] = 0. \tag{13 bis}$$

In (12) and (13) $Re = \rho(\Omega_2 - \Omega_1) d^2/\eta$ is the Reynolds number based on d and $\Omega_2 - \Omega_1$, and $\omega = \Omega_1/(\Omega_2 - \Omega_1)$ is the dimensionless velocity of the bottom disk.

Equations (4)–(12) are a system of 10 ordinary differential equations (in fact 9 since $\widehat{\theta}\widehat{\theta}_0 \equiv \widehat{R}\widehat{R}_0$ if initial conditions of both are the same), which, subject to the boundary conditions

$$g = 0 = h = h' \quad (\zeta = 0, \quad \tau > 0), \quad g = 1, \quad h = h' = 0 \quad (\zeta = 1, \quad \tau > 0), \tag{14}$$

and the initial conditions

$$g = 0 = h = h' = \widehat{ij} \quad (\tau < 0), \tag{15}$$

represent an exact solution to the flow of a Maxwellian fluid between two coaxial rotating disks. Note that the boundary conditions need not be time-independent.

2.2. Flow about a rotating disk

In the special case where there is only one rotating disk (or when $d \rightarrow \infty$), there is no natural lengthscale. However, a derived lengthscale can be defined from the angular velocity Ω of the disk, and the kinematic viscosity $\nu = \eta/\rho$ of the fluid. Thus,

instead of non-dimensionalizing all variables with respect to $\Omega_2 - \Omega_1$ and d , we non-dimensionalize them with respect to Ω and the lengthscale $(\nu/\Omega)^{\frac{1}{2}}$:

$$G = \Omega g(\zeta, \tau), \quad H = \Omega \left(\frac{\nu}{\Omega}\right)^{\frac{1}{2}} h(\zeta, \tau), \quad \zeta = \left(\frac{\Omega}{\nu}\right)^{\frac{1}{2}} z, \quad \tau = \Omega t.$$

The representations for the stresses remain the same as before, except that $\Omega_2 - \Omega_1$ and d are replaced by Ω and $(\nu/\Omega)^{\frac{1}{2}}$ respectively. The constitutive relations read exactly the same, viz (4)–(11), but with the Weissenberg number

$$Wi = \lambda\Omega.$$

However, the conservation of linear momentum requires

$$4\widehat{R}\widehat{\theta} + \widehat{\theta}\widehat{Z}' - \dot{g} - 2h'g + 2hg' = 0, \quad (16)$$

$$3\widehat{R}\widehat{R}'_1 - \widehat{\theta}\widehat{\theta}'_1 + \widehat{R}\widehat{Z}' - h' - h'^2 + g^2 + 2hh'' = 0. \quad (17)$$

Note that the radial pressure gradient is zero because the far-field conditions (at $\tau > \infty$) are quiescent. For initial conditions we again assume that the flow is at rest up to time $\tau = 0$. From then on the following boundary conditions apply:

$$\left. \begin{aligned} g = 1, \quad h = h' = 0 \quad (\zeta = 0), \\ g = 0, \quad h' = 0 \quad (\zeta = \infty). \end{aligned} \right\} \quad (18)$$

The solution of (4)–(11) and (16) and (17) subject to initial conditions (15) and boundary conditions (18) constitute an exact solution to the flow of a Maxwellian fluid about a rotating disk. Note that the solutions reported above are valid even if the boundary conditions are given by some prescribed functions of time.

3. Some asymptotic results

3.1. Small Weissenberg and Reynolds numbers

It is known that the regular perturbation solution for the steady flow of a Newtonian fluid between two coaxial rotating disks is rapidly convergent, as long as the Reynolds number is less than about 10, (Stewartson 1953). Thus we expect the perturbation solution at low Reynolds and at low Weissenberg numbers to be useful. In this limit, on expressing all variables as power series in Wi and Re we obtain

$$\begin{aligned} g = \zeta + \frac{1}{30}ReWi \{ \zeta^5 - 3\zeta^3 + 2\zeta^2 + 5\omega[\zeta^4 - 2\zeta^3 + \zeta^2] \} \\ + \frac{1}{30}Re^2 \{ -\frac{2}{21}\zeta^7 + \frac{3}{10}\zeta^5 - \frac{1}{6}\zeta^2 - \frac{4}{105}\zeta - \omega[\frac{4}{3}\zeta^5 - \frac{29}{12}\zeta^4 - \frac{3}{2}\zeta^3 + \frac{187}{60}\zeta] - 5\omega^2[\frac{1}{5}\zeta^5 - \frac{1}{2}\zeta^4 + \frac{1}{3}\zeta^3 - \frac{1}{30}\zeta] \} \\ + \text{higher-order terms,} \end{aligned}$$

$$h = -\frac{1}{60}Re \{ \zeta^5 - 3\zeta^3 + 2\zeta^2 + 5\omega[\zeta^4 - 2\zeta^3 + \zeta^2] \} + \text{higher-order terms.}$$

Of interest to the experimentalists are the radial pressure gradient, given through (13), the dimensionless torque on the top plates

$$T_t = \frac{\text{torque on top plate}}{\frac{2}{3}\pi\eta(\Omega_2 - \Omega_1)a^3/d^3} = \widehat{\theta}\widehat{Z}'|_{\zeta=1},$$

and the dimensionless torque on the bottom plates

$$T_b = \widehat{\theta}\widehat{Z}'|_{\zeta=0},$$

where a is the common radius of the disks.

Retaining only lowest-order terms, it is found that

$$\begin{aligned} p &= \left(\frac{3}{16} + \omega + \omega^2\right) Re - 2Wi, \\ T_t &= 1 + \frac{3}{700} Re^2 \left(1 - \frac{4977}{18}\omega + \frac{79}{18}\omega^2\right), \\ T_b &= 1 - \frac{2}{1575} Re^2 \left(1 + \frac{1309}{16}\omega - \frac{35}{8}\omega^2\right). \end{aligned} \quad (19)$$

For $\omega = 0$ (the bottom disk at rest) the torque experienced by the top plate is greater than that on the bottom plate. This behaviour has been noted by Griffiths *et al.* (1969), who employed a third-order fluid model.

3.2. High Weissenberg number

Under a normal operating condition of the parallel-plate viscometer most non-Newtonian fluids have a high Weissenberg number and a low Reynolds number. In the limit of high Wi and low Re the fluid behaves like an elastic solid and we feel that $g = O(1)$ and $h = o(1)$. To support this conjecture we define a new coordinate $\mu = \epsilon\zeta$, where $\epsilon = (Re/2Wi)^{\frac{1}{2}}$ in the case of two rotating coaxial disks, and $\epsilon = (2Wi)^{-\frac{1}{2}}$ in the case of one rotating disk. In the former case, assuming $g = g_0 + o(1)$ and $h = o(1)$, we have (at steady state)

$$g_0'^2 - (g_0 + \omega)^2 = \text{constant},$$

where the prime denotes a derivative with respect to μ . For $\omega = 0$ (bottom disk at rest) the solution to the above equation that has $g_0(0) = 0$ and $g_0(1) = 1$ is

$$g_0(\zeta) = \frac{\sinh(\epsilon\zeta)}{\sinh \epsilon}. \quad (20)$$

Note that the limit of $\epsilon = 0$ can be thought of as the limit of zero Reynolds number, and thus one should recover the Couette limit when $\epsilon = 0$. Furthermore, the leading terms in p and dimensionless torques are

$$\begin{aligned} p &= -2Wi \frac{\epsilon^2}{\sinh^2 \epsilon}, \\ T_t &= \frac{\epsilon}{\tanh \epsilon}, \quad T_b = \frac{\epsilon}{\sinh \epsilon}. \end{aligned} \quad (21)$$

Equation (21) is remarkably similar to (19) when ω is set to zero in the latter. The possibility of using the radial pressure gradient to measure the first normal-stress coefficient has been mentioned by Good, Schwartz & Macosko (1974). In view of the similarity between (19) and (21) this method of measuring normal-stress coefficient based on either (19) or (21) seems valid for a wide range of the Weissenberg number.

In the case of the flow about one rotating disk we find that the same governing equation for g_0 holds, except that $\omega = 0$ and $\epsilon = (2Wi)^{-\frac{1}{2}}$. The only solution that satisfies $g_0(0) = 1$ and $g_0(\infty) = 0$ is

$$g_0(\zeta) = \exp(-\epsilon\zeta). \quad (22)$$

The moment coefficient for a disk wetted on both sides can be defined as (at steady state)

$$C_M = \frac{2 \text{torque}}{\frac{1}{2}\rho\Omega^2 a^5} = -\frac{2\pi G'(0)}{a} \left(\frac{\nu}{\Omega}\right)^{\frac{1}{2}},$$

where a is the radius of the disk. In this case we have, retaining only the leading terms,

$$C_M = 2\pi(2WiRe_a)^{-\frac{1}{2}}, \quad (23)$$

where $Re_a = a^2\Omega/\nu$ is the Reynolds number based on a and Ω . Thus at high Weissenberg number the moment coefficient is inversely proportional to Ω (for a Newtonian fluid it is inversely proportional to $\Omega^{\frac{1}{2}}$). Note that the boundary-layer thickness in the limit of high Wi is of the order $(\lambda\nu)^{\frac{1}{2}}$.

3.3. Both disks rotating in the same sense

If both disks are rotating in the same sense with the same angular velocity Ω_2 , then a possible solution is $G \equiv \Omega_2$ and $H \equiv 0$ (rigid-body rotation). If $|\Omega_2 - \Omega_1|$ is small, we may express the flow variables in powers of $\alpha = (\Omega_1 - \Omega_2)/(\Omega_1 + \Omega_2)$:

$$G = \frac{1}{2}(\Omega_1 + \Omega_2) (1 + \alpha g(\zeta, \tau) + O(\alpha^2)),$$

$$H = \frac{1}{2}(\Omega_1 + \Omega_2) d(\alpha h(\zeta, \tau) + O(\alpha^2)).$$

Substituting in the governing equations and neglecting terms $O(\alpha^2)$ and higher we have (at steady state)

$$p = Re = \frac{\rho d^2(\Omega_1 + \Omega_2)}{2\eta},$$

$$h''' + 2Re g = 0, \quad (24)$$

$$g'' - 2Re h' = 0. \quad (24 \text{ bis})$$

The solution to (24) is

$$g + ih' = \frac{\sinh(Re^{\frac{1}{2}}(1-i)(\frac{1}{2}-\zeta))}{\sinh(\frac{1}{2}Re^{\frac{1}{2}}(1-i))}. \quad (25)$$

This solution is identical with the Newtonian solution given by Stewartson (1953). At high Reynolds number, (25) indicates that there will be an Ekman layer of thickness $O(Re^{-\frac{1}{2}})$ near each disk. However, if the boundary data are periodic in time with small ($O(\alpha)$) amplitude and with frequency f then it is easy to show that, at $O(\alpha)$, the constitutive equation is the familiar linear viscoelastic model. In this case the governing equations can be Fourier-transformed and it can be shown that the thickness of the Ekman layer is $O(Re^{-\frac{1}{2}})$, where now

$$Re = \frac{\rho d^2(\Omega_1 + \Omega_2)}{2\eta^*},$$

in which $\eta^* = \eta/(1 + i\lambda f)$ is the complex viscosity of the fluid. This statement can be immediately generalized to the general case of a rotating simple fluid, which has been discussed in detail by Joseph (1977). Note that at high frequency the thickness of the boundary layer is $O((\lambda f)^{-\frac{1}{2}})$.

4. Numerical solution

To support the asymptotic results we carry out numerical integrations of the governing equations for some values of the Weissenberg and the Reynolds numbers. Based on some success we have in the squeeze-film and the stagnation problems of the same fluid (Phan-Thien & Tanner 1983; Phan-Thien 1982), we treat the present problem as a time-dependent one. We use central-difference formulae for spatial derivative and employ an explicit time-integration scheme which starts at some initial conditions and stops when the flow is judged to be steady (i.e. when the value of p is unchanged to three significant figures), or when time τ is greater than 20. On the ζ -axis ($0 \leq \zeta \leq l$, where $l = 1$ for the coaxial-disk flow, and l is of order 5–10, depending on the Weissenberg number, for the flow about a rotating disk) we select

equispaced nodal points at $\zeta_i = (i - 1)\Delta h, i = 1, \dots, N + 1$, where $\Delta h = l/N, N$ being the number of intervals from 0 to l . Second-order finite-difference formulae for ζ -derivatives are employed for each field variable. At $\zeta = 0$ and at $\zeta = l$ we impose the boundary conditions (14) or (18). For the coaxial-disk flow problem we have from (13 bis) (denoting by ψ_i^n the value of the field variable ψ at time $\tau = n\Delta\tau$ and at $\zeta = \zeta_i$)

$$\sum_{j=1}^{N-1} A_{ij} h_j^n = \text{a known } (N-1) \text{ vector,}$$

where **A** is the Rouse $[N - 1, N - 1]$ matrix

$$A_{ij} = \begin{cases} 2 & (i = j), \\ -1 & (i = j \pm 1). \end{cases}$$

Since the inverse of the Rouse matrix is the Kramers matrix

$$C_{ij} = \begin{cases} i(N-j)/N & (i \leq j), \\ j(N-i)/N & (j \leq i). \end{cases}$$

The equations for h_j^n can be inverted to give h_i^n . To update the field variables (g, h' and the stresses for the flow about a rotating disk; h is then found by a trapezoidal rule from h') we employ the following explicit schemes: if

$$\dot{\psi}_i = f_i(\psi, \tau)$$

then ψ_i is updated using

$$\psi_i^{n+1} = \psi_i^n + \Delta\tau [\alpha_1 f_i(\Psi^n, \tau) + \alpha_2 f_i(\bar{\Psi}, \tau + \Delta\tau)],$$

where $\bar{\Psi} = \Psi^n + \Delta\tau \mathbf{f}(\Psi^n, \tau)$. For $\alpha_1 = 1$ and $\alpha_2 = 0$ the scheme is the classical first-order Euler method which is accurate to $O(\Delta\tau)$ and requires only one derivative evaluation per time step. For $\alpha_1 = \alpha_2 = \frac{1}{2}$ we have the second-order Huen method, which is accurate to $O(\Delta\tau^2)$ but requires two derivative evaluations per time step. Most results reported in this section were obtained using Huen's method ($\Delta\tau \approx 0.01-0.001$ and $\Delta h = 0.1-0.02$). All calculations were done on a Cyber machine that retains 15 significant figures.

To evaluate the dimensionless radial pressure gradient for the coaxial-disk flow we find that a straightforward finite-difference solution of equation (13) is very inaccurate. A better way to compute the spatial average of (13) is

$$p = \int_0^1 (3\widehat{R}\widehat{R}_1 - \widehat{\theta}\widehat{\theta}_1 + Re[(g + \omega)^2 - 3hh'']) d\zeta + \widehat{RZ}|_{\zeta=1} - \widehat{RZ}|_{\zeta=0}.$$

4.1. Coaxial-disk flow

Starting the numerical scheme at the initial conditions (15), we find that the steady-state solution for small Weissenberg and small Reynolds numbers ($Wi \leq 1, Re \leq 2$) is substantially as predicted by the perturbation solution. In fact, at $Wi = 1$ and $Re = 2$ the perturbation solution predicts that the dimensionless radial pressure gradient should be $-1.4 + O(Re^2, Re Wi, Wi^2)$, whereas our numerical solution shows $p = -1.36$. We show in figure 1 the steady-state velocity field at a Weissenberg number of 1 and different Reynolds numbers up to 50. Note that at high Reynolds number and low Weissenberg number there is a thin boundary layer near the rotating disk, and the bulk of the fluid is at rest. The flow in this limit is qualitatively similar to that of a Newtonian fluid, which has been discussed by Stewartson (1953).

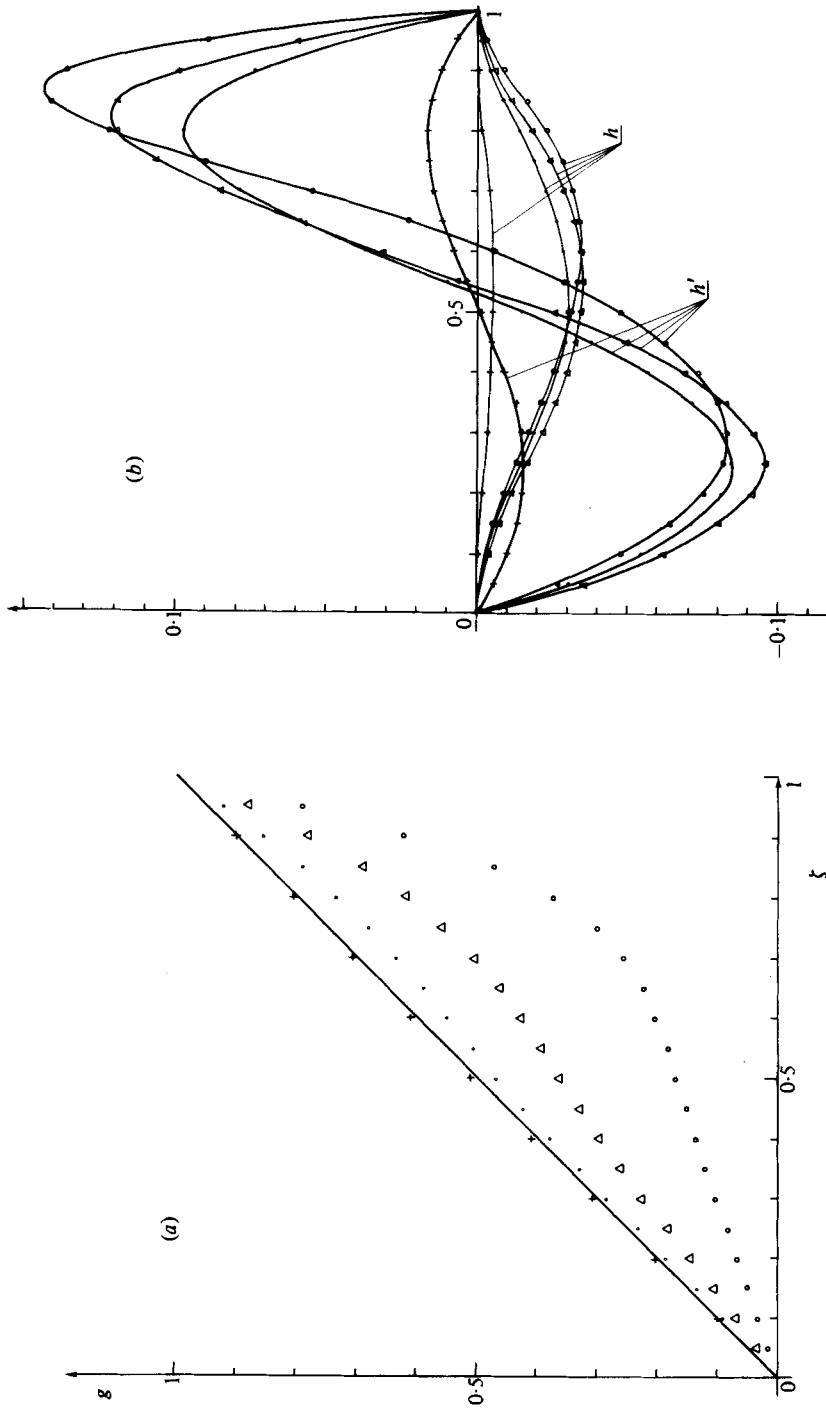


FIGURE 1. (a) Steady-state angular velocity for the coaxial-disk flow at a Weissenberg number of 1 and at different Reynolds numbers: —, $Re = 0$; +, 1; ●, 10; △, 20; ○, 50. (b) Secondary flow h and h' for the coaxial-disk flow at $Wi = 1$. Symbols as in (a).

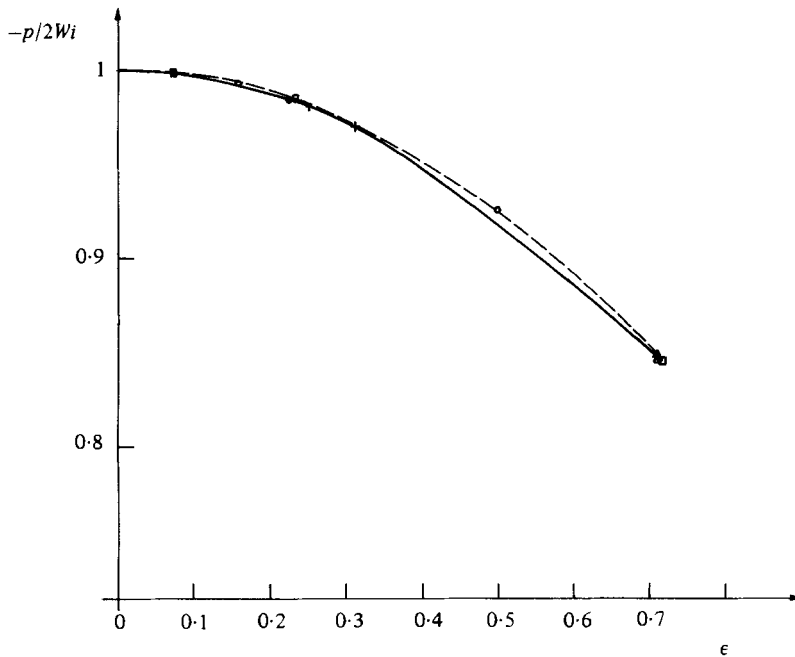


FIGURE 2. Dimensionless radial pressure gradient $-p/2Wi$ at different values of $\epsilon = (Re/2Wi)^{1/2}$: —, asymptotic solution (small ϵ); ---, regular perturbation solution (small Re and small Wi). Numerical data: \triangle , $Wi = 0.1$; +, 0.5 ; \bullet , 1 ; \circ , 2 ; \square , 10 .

At high Weissenberg number and low Reynolds number, in the sense that $\epsilon = (Re/2Wi)^{1/2}$ is small, we have the asymptotic results (20) and (21). We find that (20) describes the velocity well for values of ϵ up to 0.3 (the largest Weissenberg number that still maintains the stability of our numerical scheme is 10). However, even at a value of $\epsilon = 0.7$ ($Re = Wi$) and at $Wi = 10$ the asymptotic formula (21) for p remains extremely accurate (see figure 2), although the velocity field cannot be described accurately by (20). Thus it seems that as far as pressure measurements are concerned the simple formulae (19) or (21) are accurate enough for a wide range of Weissenberg number provided that $\epsilon = (Re/2Wi)^{1/2}$ is less than 0.7, or that both the Weissenberg and the Reynolds number are small ($Wi \leq 1$, $Re \leq 2$).

4.2. Flow about a rotating disk

Based on the Newtonian solution (Cochran 1934) we choose $l = 5$ for $Wi \leq 1$. Steady-state solution can be obtained without any numerical problem for $Wi \leq 1$ and these results are displayed in figure 3. At high Weissenberg number our asymptotic result (22) indicates that the bulk of the fluid will rotate as a rigid body. (This is not a surprising result, since in this limit the fluid behaves like an elastic solid.) Thus for Wi from 1 to 10 we choose $l = 10$. For impulse-started initial conditions ($g = 1$ at $\zeta = 0$ and $t \geq 0+$) it is clear that the fluid transmits a transverse wave which propagates through the flow field. From Tanner's (1962) solution of the Rayleigh problem we expect that the transverse wave speed is $Wi^{-1/2}$. This agrees well with the numerical solutions. In figures 4 and 5 we plot the angular velocity at different times for two values of the Weissenberg number. To capture these waves accurately, the spatial discretization must be small ($\Delta h \approx 0.02-0.01$), and therefore the computing time is rather long (the information displayed in figure 5 took approximately 1 h of

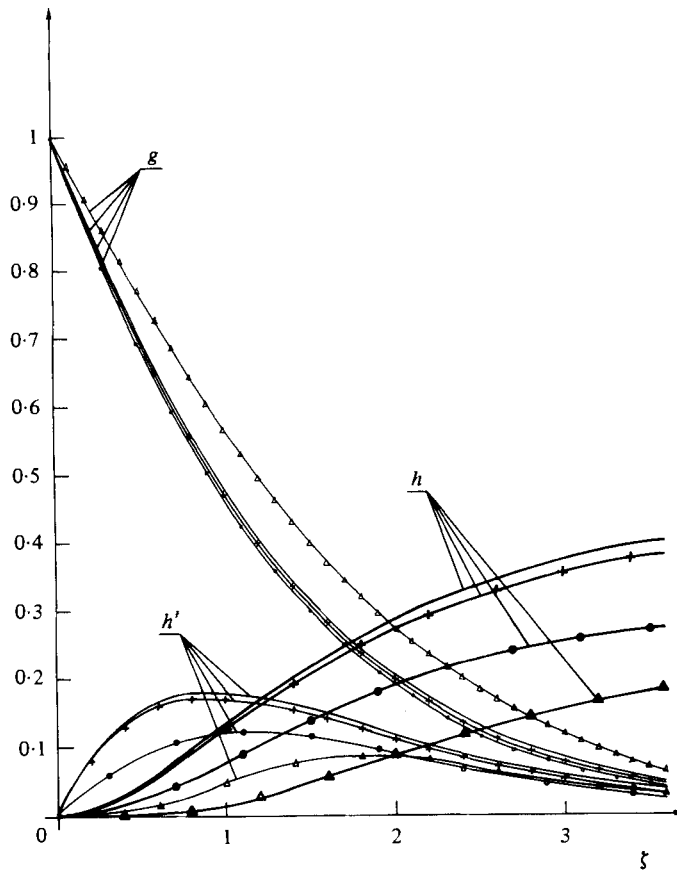


FIGURE 3. Steady-state velocities for the flow about a rotating disk: —, $Wi = 0$; +, 0.1; O, 1; Δ , 2. The boundary-layer thickness first decreases and then increases with Wi . The magnitude of the secondary flow decreases with Wi .

computing time on the Cyber). To overcome this problem partly the angular velocity of the disk can be slowly increased from 0 to 1. We adopt the simple time-dependent angular velocity $g(0) = \tau/Wi$, $0 \leq \tau \leq Wi$ and $g(0) = 1$, $\tau > Wi$. The slope of the shear wave is roughly $-Wi^{-\frac{1}{2}}$ and the spatial discretization can be increased to 0.05. In figure 6 we show the time evolution of the angular velocity at a Weissenberg number of 10. For this case the boundary layer (distance for which g decays to 0.1) is roughly 10, from the asymptotic solution (22). The viscoelastic waves will have implications in numerical schemes that employ a timelike integration of the constitutive equations. In these schemes any numerical noise will propagate and reflect from the boundaries as waves, and it is not inconceivable that at high Weissenberg number (remembering that the wave speed is proportional to $Wi^{-\frac{1}{2}}$) the wave will persist for a long time, which tends to produce more numerical noise and eventually destroys the convergence of the scheme. Finally, of interest to the experimentalist is the moment coefficient for a rotating disk wetted on both sides. On figure 7 we plot $C_M Re_a^{\frac{1}{2}}$, where $Re_a = \rho\Omega a^2/\eta$ is the Reynolds number based on the radius a of the disk, versus the Weissenberg number. The Newtonian value 3.87 and the asymptotic result (23) are also shown on the graph. It is remarkable that the asymptotic result (23) is extremely accurate for $Wi \geq 1$ ($\epsilon = (2Wi)^{-\frac{1}{2}} \leq 0.7$). Since both Re_a and Wi are

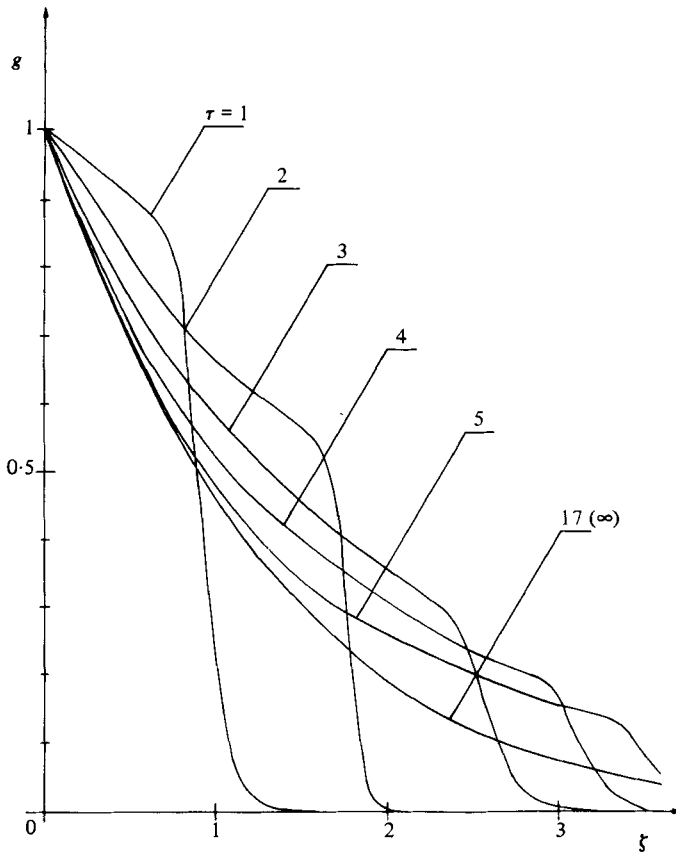


FIGURE 4. Time-dependent angular velocity at $Wi = 1$. The flow is impulsively started. Note that the traversed wave speed is approximately 1.

proportional to the angular velocity Ω one should see a transition from $C_M \propto \Omega^{-\frac{1}{2}}$ for Newtonian fluid to $C_M \propto \Omega^{-1}$ for highly elastic fluid. This transition occurs at a Weissenberg number of unity and should be subjected to experimental verification.

5. Final remarks

It is worthwhile mentioning that the Kármán's solution (3) is also an exact solution to the second-order fluid model. Since the steady coaxial-disk flow of this fluid has been studied by Bhatnagar & Zago (1978) and since it has some unpleasant stability properties in unsteady flows, we shall not carry out the full numerical solution here. Instead, we note that the counterpart of (19) is

$$\frac{1}{r} \frac{\partial P}{\partial r} = \frac{3}{10} \rho \Omega^2 - (\nu_1 + \nu_2) \frac{\Omega^2}{d^2} + O(\Omega^4),$$

where $\nu_i, i = 1, 2$, are the normal-stress coefficients. Thus if the centre of the top plate is connected to a small open tube then the fluid will rise in the tube to a height of

$$-\frac{3}{20} \frac{\Omega^2 a^2}{g} + (\nu_1 + \nu_2) \frac{\Omega^2 a^2}{2 \rho g d^2} + O(\Omega^4),$$

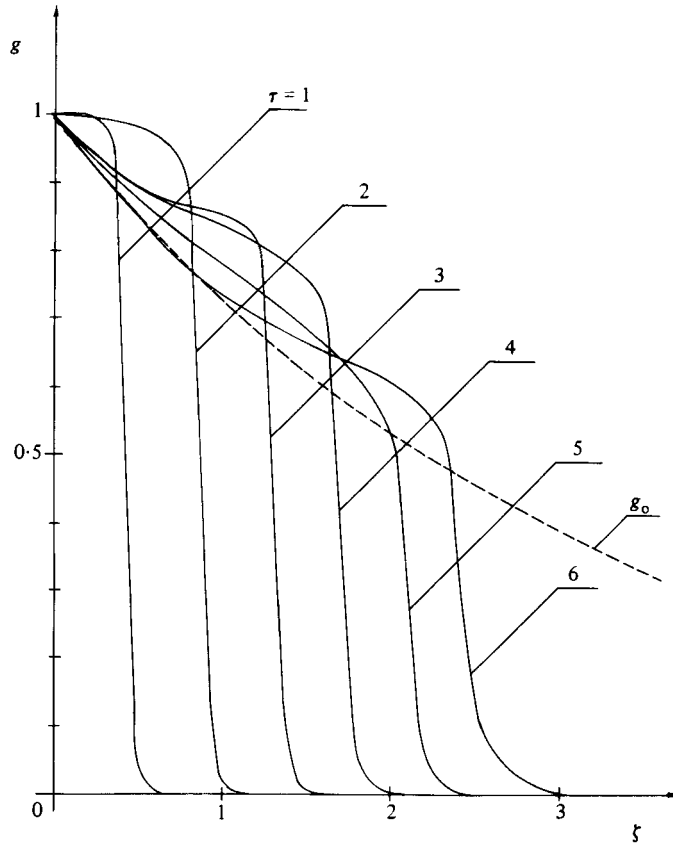


FIGURE 5. Same as in figure 4, but at $Wi = 5$. The traversed wave speed is approximately $0.45 \approx 5^{-\frac{1}{2}}$.

where g is the acceleration due to gravity. This centripetal pumping effect has been suggested as a method to measure normal stress coefficients (see e.g. Good *et al.* 1974), but its use in rheometry has not yet been investigated in detail. Furthermore, with a slight modification to the representation for the stresses† (Williams 1976), it can be shown that Kármán's solution is an exact solution to the Oldroyd fluid B . This fluid has a diffusive mechanism (retardation) and cannot transmit waves (Tanner 1962). Our unsteady numerical scheme reported in this paper is expected to perform well with this model fluid.

However, the stress representation of Williams (1976) is not an exact solution to either the corotational model (lower-convective Maxwell model) or the Oldroyd 4-constant model (for a summary of these models see Bird, Armstrong & Hassager 1977). To substantiate this remark, let us briefly consider the Oldroyd 4-constant model where the stress tensor \mathbf{S} is related to the velocity-gradient tensor \mathbf{L} by

$$\mathbf{S} + \lambda \frac{\delta}{\delta t} \mathbf{S} + 2\mu(\text{tr } \mathbf{S}) \mathbf{D} = 2\eta \mathbf{D} + 2\theta \frac{\delta}{\delta t} \mathbf{D},$$

† This stress representation is identical with ours, with the exception that S_{zz} contains an additional term which is quadratic in r .

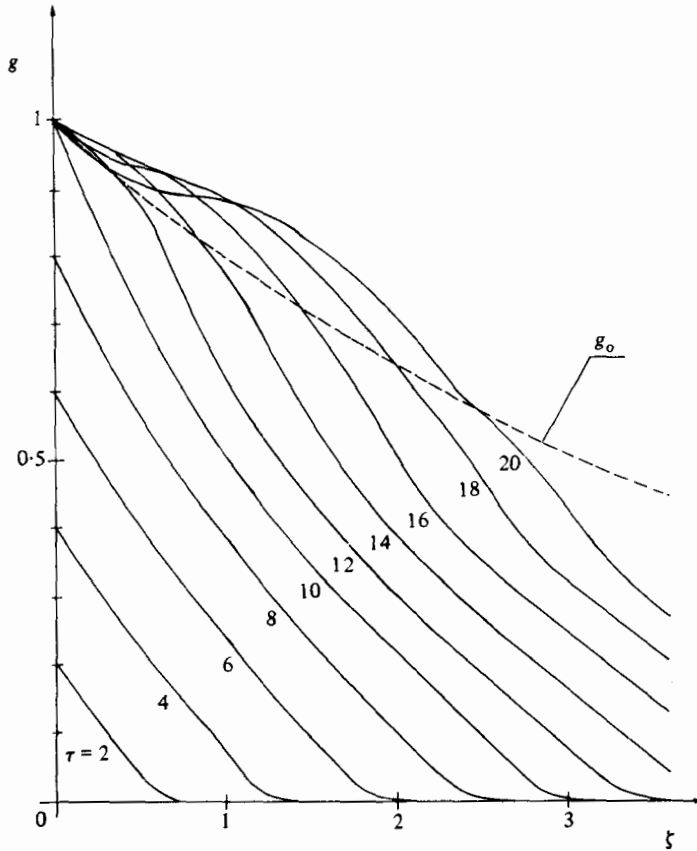


FIGURE 6. Time-dependent angular velocity at $Wi = 10$. The angular velocity of the disk is taken to be 0.1τ for $\tau \leq 10$. From then on it remains constant at a value of 1. The slope of the shear wave is approximately $-(Wi)^{-1/2}$.

where
$$\frac{\delta}{\delta t} \mathbf{A} = \partial_t \mathbf{A} + \mathbf{u} \cdot \nabla \mathbf{A} - \mathbf{L} \mathbf{A} - \mathbf{A} \mathbf{L}^T$$

is the upper convective derivative, and μ and θ are two new material parameters; other symbols have the same meaning as in (1). Assuming Kármán's velocity field (3), one sees at once that the components of the stress tensor must be full power series in the radius. For instance, the equation for $S_{\theta z}$ reads

$$S_{\theta z} + \lambda(\partial_t S_{\theta z} + rH' \partial_r \theta_{\theta z} - 2H \partial_z S_{\theta z} + H' S_{\theta z} - rG' S_{zz}) + \mu(S_{rr} + S_{\theta\theta} + S_{zz}) rG' = \eta rG' + \theta r(\partial_t G' + 6H'G' - 2HG''),$$

where the prime denotes a z -derivative. If one adopts Williams' stress representation as in the work of Bhatnagar & Perera (1982), it then follows that the term $(S_{rr} + S_{\theta\theta} + S_{zz}) rG'$ must be cubic in r , because $\text{tr} \mathbf{S}$ is quadratic in r . To balance this term, $S_{\theta z}$ must contain a cubic term in r . Since the equations for $S_{r\theta}$ and $S_{\theta\theta}$ contain a term $rS_{z\theta}$, $S_{r\theta}$ and $S_{\theta\theta}$ must have a quartic term in r and so on. Thus one finds that, assuming Kármán's velocity field, the stresses are given by

$$\{S_{rr}, S_{r\theta}, S_{\theta\theta}, S_{zz}\} = \sum_{n=0}^{\infty} r^{2n} \{\widehat{R}R_n, r^2 \widehat{R}\theta_n, \widehat{\theta}\theta_n, \widehat{Z}Z_n\},$$

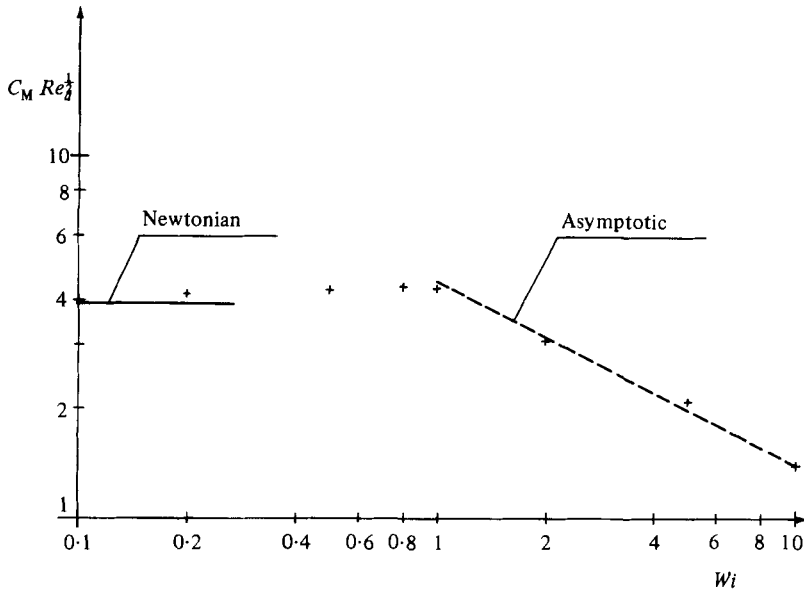


FIGURE 7. Moment coefficient $C_M Re_a^{1/2}$ versus the Weissenberg number: —, Newtonian value; ---, asymptotic result. At low values of Wi , $C_M Re_a^{1/2}$ remains roughly constant. At high values of Wi ($Wi \geq 1$), $C_M Re_a^{1/2}$ is given by $(2Wi)^{-1/2}$.

$$\{S_{rz}, S_{\theta z}\} = \sum_{n=0}^{\infty} r^{2n+1} \{\widehat{RZ}_n, \widehat{\theta Z}_n\},$$

where \widehat{ij}_n are some functions of z and t .

Since the convergent properties of these power series in r have not been investigated, Bhatnagar & Perera's numerical results can only be best viewed as a perturbation solution about r . Similar series representation for the stresses can be shown for the corotational model or the 'non-affine' network model, which employs a mixture of the upper- and lower-convective derivative. Note that, if $\mu = 0$, then the series terminate and one obtains Williams' solution for the stresses.

It is a pleasure to acknowledge the support of the Australian Research Grant Scheme (ARGS F79 15597 R). The author wishes to thank Professor Gary Leal at the Department of Chemical Engineering at Caltech for providing a hospitable atmosphere.

REFERENCES

BATCHELOR, G. K. 1951 *Q. J. Mech. Appl. Math.* **4**, 29.
 BENTON, E. R. 1966 *J. Fluid Mech.* **24**, 781.
 BHATNAGAR, R. K. & ZAGO, J. V. 1978 *Rheol. Acta* **17**, 557.
 BHATNAGAR, R. K. & PERERA, M. G. N. 1982 *J. Rheol.* **26**, 19.
 BIRD, R. B., ARMSTRONG, R. C. & HASSAGER, O. 1977 *Dynamics of Polymeric Liquids*, vol. I. Wiley.
 BOGER, D. V. 1977/78 *J. Non-Newton. Fluid Mech.* **3**, 87.
 COCHRAN, W. G. 1934 *Proc. Camb. Phil. Soc.* **30**, 365.
 GRIFFITHS, D. F., JONES, D. T. & WALTERS, K. 1969 *J. Fluid Mech.* **36**, 161.
 GOOD, P. A., SCHWARTZ, A. J. & MACOSKO, C. W. 1974 *A.I.Ch.E. J.* **20**, 67.

- HOLODNIOK, M., KUBÍČEK, K. & HLAVÁČEK, V. 1977 *J. Fluid Mech.* **81**, 689.
- JOSEPH, D. D. 1977 *Arch. Rat. Mech. Anal.* **66**, 311.
- KÁRMÁN, T. VON 1921 *Z. angew. Math. Mech.* **15**, 191.
- PEARSON, J. R. A. 1982 *Computer Methods in Chemical Engineering*. Applied Science Publishers.
- PHAN-THIEN, N. & TANNER, R. I. 1983 *J. Fluid Mech.* **129**, 265.
- PHAN-THIEN, N. 1982 *Rheol. Acta* (in press).
- RATHNA, S. L. 1962 *Z. angew. Math. Mech.* **42**, 231.
- STEWARTSON, K. 1953 *Proc. Camb. Phil. Soc.* **49**, 333.
- TANNER, R. I. 1962 *Z. angew. Math. Phys.* **13**, 573.
- WALTERS, K. 1975 *Rheometry*. Chapman & Hall.
- WILLIAMS, E. W. 1976 *J. Non-Newt. Fluid Mech.* **1**, 51.